ELSEVIER

Chemical Engineering Journal 82 (2001) 87–94

Chemical Engineering Journal

www.elsevier.com/locate/cej

A simple adsorber dynamics approach to simulated countercurrent moving bed reactor performance

Shuiyuan Huang, Robert W. Carr*

Department of Chemical Engineering and Materials Science, University of Minnesota, 421 Washington Ave. S.E., Minneapolis, MN 55455, USA

Received 8 May 2000; accepted 6 November 2000

Abstract

The design and performance of a simulated countercurrent moving bed chromatographic reactor (SCMCR) for high temperature reactions are investigated for both reversible and irreversible reactions of a single reactant. From an analysis of the solid phase and gas phase flow ratios in each of the SCMCR sections, the flow conditions necessary for optimizing the conversion and yield are obtained. Reactor performance is not evaluated from typical material balance equations, but rather by considering the separation of reactant and product waves as they flow through the sections of the SCMCR, and as the feed point is cycled under the assumption of dispersionless plug flow. The additional assumptions of linear adsorption equilibria and infinite gas–solid mass transfer rates permit the expressions for exit molar flow profiles during the initial transient period, and of the ultimate periodic steady state, to be readily obtained. Simple algebraic expressions for the production rate of the reaction product as a function of the adsorption equilibrium constants, the per pass conversion, the number of switching periods, and the molar flow rate of the reactant, are presented.

Keywords: SCMCR; Reactor performance; Per pass conversion

1. Introduction

The simulated countercurrent moving bed chromatographic reactor (SCMCR) embodies the integration of adsorptive separation with chemical reaction [1]. Experimental implementations of this type of separative reactor have shown great improvement in conversion and in product purity compared to the same reactions carried out in conventional reactors. When reactant conversion is limited by chemical equilibrium, the SCMCR permits the equilibrium to be shifted in the direction of products, giving greatly enhanced conversion [2–5]. Similarly, for reactions which have an intrinsically low conversion per pass in conventional reactors, the SCMCR permits substantially enhanced conversion [6,7]. Several mathematical models have been developed for SCMCR configurations in which reaction and separation are locally integrated by mixing catalyst and adsorbent or by other means [8–13].

Bjorklund and Carr [14] have discussed the development of SCMCR design for high temperature reactions. It is very common that to attain an adequate reaction rate the reaction temperature must be significantly above the range where adsorptive separations are possible. In this case, it is possible to configure the SCMCR as in Fig. 1, where a high temperature reactor is followed by lower temperature adsorbers. In this case, the flow switching operations that are characteristic of simulated countercurrency are designed to successively place the reactor before each section of a simulated moving bed separator as the feed is switched in the direction of carrier flow. Although reaction and separation take place successively, the combination of reactor followed by adsorber performs the same function as when reaction and separation are integrated, for example, by mixing a catalyst and an adsorbent. While the per pass conversion in a single section cannot be improved with this in-series arrangement, the *overall* conversion attained by the SCMCR can be significantly better than conventional non-separative reactors.

The general principles for design and performance of the SCMCR shown in Fig. 1 are needed. Two mathematical models of SCMCR designs for the high temperature (∼1000 K) methane oxidative coupling reaction have been reported [15,16]. These differ from the models for locally integrated reaction and separation referenced above. They are models based on differential material balance equations, and they are specifically for simulating experimental observations of oxidative coupling reactor performance [6,7,17]. As such they are not sufficiently general to be more broadly useful. In this paper we present a model for a high temperature

* Corresponding author. Tel.: +1-612-625-2551; fax: +1-612-626-7246.
E-mail address: carrx002@tc.umn.edu (R.W. Carr).

1385-8947/01/$ – see front matter
PII: S1385-8947(00)00356-9

Nomenclature

A	separation column cross-sectional area (m^2)
F	molar flow rate (mol/s)
G	gas volume flow rate (m^3/s)
K_P	adsorption equilibrium constant of product
K_R	adsorption equilibrium constant of reactant
L	column length (m)
n	sequence of switching period
P	product
R	reactant
S	solids pseudo-flow rate (m^3/s)
t_{bP}	the breakthrough time of P (s)
t_{bR}	the breakthrough time of R (s)
U_g	gas phase flow speed (m/s)
U_s	solid phase flow speed (m/s)
X	conversion

Greek letters

α	separation factor
ε	column porosity
σ	ratio of solid phase adsorbate mass flow rate to gas phase adsorbate mass flow rate
τ	switching period (s)

Subscripts

0	inlet
m	make-up feed
n	switching period rank
P	product
R	reactant

SCMCR that is of general utility, and furthermore, is readily and easily applied.

The approach is based on the ideal model, in which axial dispersion and mass transfer resistances are neglected, and adsorption is described by linear isotherms. The analysis of simulated moving bed chromatography (no reactions) with the linear, ideal model has analytical solutions [18]. Similarly, the model developed below results in analytical expressions, but relatively simple ones, for SCMCR performance. The optimal flow conditions of the SCMCR are first set down, and then the reactor performance is analyzed. The analysis is not based on the solutions to the usual differential material balance equations, but rather on algebraic material balances and the adsorptive separation of reactant and product as these species flow about the SCMCR. Rectangular matter waves are formed by the flow switching operations. Their movement forms an insightful dynamical picture of reactor operation. One can see the development of the initial transient period, and its approach to the periodic steady state that is characteristic of simulated moving beds. Simple algebraic expressions for the dependence of reactor performance on per pass conversion, adsorption equilibrium constants, and reactant concentration are presented.

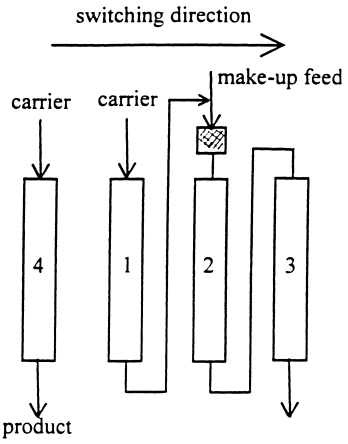

Fig. 1. Schematic of the SCMCR. Cross-hatched unit is a high temperature reactor. Numbered units are adsorbers.

2. Flow rate criteria for SCMCR design

The SCMCR is schematically represented in Fig. 1. It is of the type developed for high temperature reactions, in which the separations must be carried out at a lower temperature. It consists of four adsorption columns and a reactor, although in principle, any number of columns can be used. Four columns are usually required provided the separation is not difficult. If more adsorbers are needed, they are added and those performing the same function are grouped in series and called a section. Four sections are normally necessary. In the following, the four columns performing the different functions will be spoken of interchangeably as sections and as columns. In Fig. 1 the reactor is crosshatched, and the adsorbers are numbered to facilitate discussion. To simulate countercurrent flow the carrier inlets, reactant make-up feed, and product take-off point, as well as the reactor are all advanced by one column in the direction of fluid flow at fixed time intervals, called switching periods. The numbering of each column is also advanced one column to the right at each feed advancement.

The SCMCR is closely related to the countercurrent moving bed reactor, with a fluid flow speed, U_g, and a pseudo-solids flow speed, U_s, in each section given by

$$U_s = \frac{L}{\tau}, \qquad U_g = \frac{G}{\varepsilon A} \tag{1}$$

where L is the length of an adsorption column, τ the switching period, G the volume flow rate of fluid phase, ε the void fraction of the adsorption column, and A is the column cross-sectional area. A chemical reaction, given by Eq. (2), occurs and requires a high enough temperature so that the configuration of Fig. 1 should be implemented.

$$R \rightarrow P \tag{2}$$

The adsorption isotherms of both R and P are linear, $q_i = K_i C_i$. (In SCMCR operation the carrier flow rates may be much larger than the make-up feed flow rate, and R and P may be sufficiently diluted with the carrier gas that their isotherms can be approximated as linear.) The model also assumes local adsorption equilibrium, and that P is more strongly adsorbed than R, i.e. $K_P > K_R$.

With this ordering of the magnitude of K_P and K_R, the switching period and mobile phase flow rate can be chosen so R flows through the sections at the same rate that the feed point is advanced, and the more strongly adsorbed P lags behind it. The parameter that governs the movement of the concentration front of any species i in a countercurrent mass transfer process with a linear isotherm is σ_i [19,20].

$$\sigma_i = \frac{K_i S}{G} = \frac{(1-\varepsilon)}{\varepsilon}\left(\frac{U_s}{U_g}\right) K_i \tag{3}$$

When $\sigma_i > 1$ the net flow of the ith adsorbate is in the direction of solid flow, and when $\sigma_i < 1$ the net flow of the ith adsorbate is in the direction of fluid flow. When $\sigma_i = 1$ equal amounts of the adsorbate are carried in opposite directions by the countercurrent flow of adsorbent and carrier gas.

In order to obtain a high conversion only minimal amounts of R should be permitted to exit the reactor in either the product stream or in the carrier stream of Fig. 1. The optimal operating condition with respect to conversion is to set the flow rates so that no R is lost, and all P emerges in the product stream. If this can be done, 100% conversion can be attained, as can a product stream that is uncontaminated by R. In practice, this may be difficult to achieve. Optimal flows are obtained by applying Eq. (3) to each section of the SCMCR. In section 1, U_s and U_g should be set so that $\sigma_R \leq 1$, and $\sigma_P > 1$, and in sections 2 and 3, $\sigma_R \geq 1$. According to Eq. (3) and the assumption that $K_P > K_R$, $\sigma_P > 1$ when $\sigma_R \geq 1$ in sections 2 and 3. The product can be taken from the SCMCR at section 4 by purging with extra carrier gas. To simplify the following discussion, it is assumed that section 4 does not contain any R or P at the end of any switching period. Therefore, the flow rate of P in the fluid phase of section 4 should not be less than in the solid phase, i.e. $\sigma_P \leq 1$. According to Eq. (3) and the assumption that $K_P > K_R$, $\sigma_R < 1$ when $\sigma_P \leq 1$ in section 4. Thus, the operating conditions are as follows:

$$\begin{aligned}
&\text{section 1}: \quad \sigma_R \leq 1.0, \quad \sigma_P > 1.0\\
&\text{section 2}: \quad \sigma_R \geq 1.0, \quad \sigma_P > 1.0\\
&\text{section 3}: \quad \sigma_R \geq 1.0, \quad \sigma_P > 1.0\\
&\text{section 4}: \quad \sigma_P \leq 1.0
\end{aligned} \tag{4}$$

Note that the flow rates of solid and fluid in section 2 are equal to those in section 3, and that these two sections operate under the same conditions.

Since the countercurrent flow in the SCMCR is simulated by using a multiple section fixed-bed system with an appropriate sequence of column switching, the solids pseudo-flow rates in all four sections are equal. The carrier gas flow rate in sections 1–3 are approximately equal if the make-up feed flow rate is negligibly small in comparison with the carrier gas flow. Substituting the σ_i in the set of inequalities (4) with the corresponding $K_i S/G$, gives

$$\begin{aligned}
&\text{section 1}: \quad \frac{K_R S}{G} \leq 1.0, \quad \frac{K_P S}{G} \geq 1.0\\
&\text{sections 2 and 3}: \quad \frac{K_R S}{G} \geq 1.0\\
&\text{section 4}: \quad \frac{K_P S}{G_4} \leq 1.0
\end{aligned} \tag{5}$$

The above set of inequalities (5) has an optimal solution. For sections 1–3, the common flow rate ratio in this set of inequalities is

$$\frac{K_R S}{G} = 1.0 \tag{6}$$

For section 4, the optimal carrier gas flow rate, i.e. the least value of G_4, is given by

$$\frac{K_P S}{G_4} = 1.0 \tag{7}$$

although in practice, it is usually necessary to use a higher gas flow rate in section 4 in order to insure complete purging. For the SCMCR shown in Fig. 1, the solids volume pseudo-flow rate S is

$$S = \frac{LA(1-\varepsilon)}{\tau} \tag{8}$$

Upon substitution of S into Eq. (6), the switching period is obtained as Eq. (9), and it is evident that the switching period, τ, equals the breakthrough time of R, t_{bR}.

$$\tau = t_{bR} = \frac{LA(1-\varepsilon)K_R}{G} \tag{9}$$

In general, there are four parameters in a separation section of the SCMCR, G, L, A and τ. When any three of them are given, the remaining one can be obtained from Eq. (9). After the solids pseudo-flow rate, S, is determined in sections 1–3, the carrier gas flow rate in section 4 can also be obtained by Eq. (7).

3. Development of composition distribution

In this section, equations for the development of reactant and product composition distribution within the SCMCR are deduced from considerations of the molar flow rates of reactant and product. The reactant enters the SCMCR as a rectangular wave, where the leading edge is created when the feed is switched into the current feed section, and the trailing edge is formed when the reactant flow is terminated at the end of a switching period. If the valve action is rapid, the leading and trailing edges can be considered to be step functions. Furthermore, since the isotherm is linear, the flow

is dispersionless, and since mass transfer rates are fast, the shape of the composition wave is not altered as it travels through the SCMCR. Let the SCMCR shown in Fig. 1 be initially filled only with carrier gas, and then started by introducing feed into the chemical reactor, which is initially placed at section 2. The profiles of R and P that develop as the feed point cycles through the SCMCR will be examined. There will be an initial transient period, possibly taking several cycles, that finally evolves into a periodic steady state. The analysis that follows is based solely on conversion per pass and requires no information about the nature of the chemical reactor, or about the reaction kinetics. These are not needed for the present modeling approach. They are important issues that should be investigated separately to optimize per pass conversion and selectivity. The results of such a study can be readily incorporated into the SCMCR model. The irreversible reaction will be examined first, then the reversible reaction will be considered.

3.1. The irreversible reaction

Although the SCMCR is frequently only considered for reversible, equilibrium-limited reactions, it is also very useful for low conversion per pass reactions, such as methane oxidative coupling [6,16], which may be considered to be irreversible. With reference to Fig. 1, we start with column 2, and qualitatively examine the evolution of the composition distribution during the first four switching periods (the first cycle). In the first switching period, section 2 receives the reactor effluent and adsorbs both unconverted R and the product, P. The R breaks through the outlet of section 2 as the first switching period is terminated, while the more strongly adsorbed P has only advanced part way along the adsorber. In the second switching period, this column occupies section 1 and is swept with carrier gas. For a linear isotherm, the desorption time (the time taken for a saturated column to be swept clean) is equal to the breakthrough time provided the carrier flow rate is unchanged. Therefore, R is swept from section 1 at the end of the second switching period. In the third period, this column moves into the section 4 position. It is devoid of R now, but still contains P. When the breakthrough time ratio of P to R is greater than 2, i.e. $K_P/K_R \geq 2$, P does not break through section 1 in the second switching period. When $1 < K_P/K_R < 2$, a portion of P is swept out of section 1 and forward into the reactor in section 2 during the second switching period. No matter what the ratio of K_P/K_R is, section 4 contains no R and P at the end of the third switching period when the carrier gas flow rate in section 4 is not less than G_4 as given by Eq. (7). In the fourth switching period, this column moves into the section 3 position, and contains no R and P because neither one is permitted to break through section 2.

The reactant flow in the reactor feed is composed of two parts; make-up feed which has fixed composition, and unreacted R from section 1. The make-up feed rate is adjusted so that the molar feed flow rate of R entering the reactor is F_{R0} for every switching period. Thus, the reactor effluent always has the composition $F_R = F_{R0}(1 - X)$, where X is the per pass conversion. The molar flow rate of P formed by reaction is then given by $F_P = F_{R0}X$. However, the flow rate of P may be greater than this if P enters the reactor from upstream (see below).

3.1.1. First switching period

The SCMCR start-up commences with the first switching period. During the first period, the flows of R and P coming from section 1 are zero. Reactant R is fed into the reactor only from the make-up, which during the first switching period has the flow rate F_{R0}, and is different from all later periods. Reactant R and product P exit from the reactor and are carried into the section 2 adsorber bed. At t_{bR}, the feed and draw-off ports, as well as the reactor effluent are shifted to the next column in the direction of carrier gas flow, the first switching period ends, and the second switching period starts, simultaneously. At the end of the first switching period, the distributions of R and P in section 2 are as shown in Fig. 2. Sections 1, 3 and 4 do not yet contain R and P. The molar flows of R and P exiting the reactor and entering the adsorber are $F_R = F_{R0}(1 - X)$ and $F_P = F_{R0}X$.

3.1.2. Second switching period

During the second switching period, unconverted R emerging from section 1 (the former section 2) is mixed with make-up feed so that the flow rate entering the reactor is F_{R0}, the same as during the first switching period. Since the desorption time equals the breakthrough time, the flow rate of R in the stream from section 1 during the entire switching period is $F_{R0}(1-X)$. When $K_P/K_R \geq 2$, the flow of P in the feed during the second switching period is 0; but when $1 < K_P/K_R < 2$, a portion of P is swept from section 1 and into the reactor. Fig. 2 shows the flow rate profiles in section 2 at the end of the first switching period for the case $1 < K_P/K_R < 2$. This is also the profile in the first section at the beginning of the second switching period. It is apparent from Fig. 2 that there is a time interval at the beginning of the second switching period when no P enters the reactor. This is shown in Fig. 3, which plots flow rates in section 1 versus time during the second switching period. The R is completely desorbed at $t = \tau$, while the slower moving P breaks through at $t_{bP} - t$. The portion of P swept into the reactor during the second switching period is represented by the block between t_{bP} and t. The remaining portion of

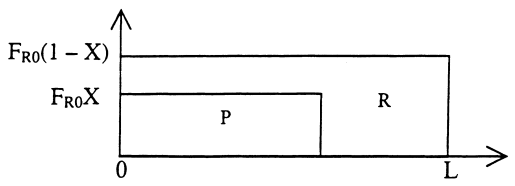

Fig. 2. The profiles of R and P in section 2 at the end of the first switching period ($1 < K_P/K_R < 2$).

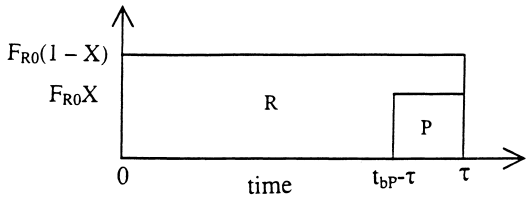

Fig. 3. The recycling feed composition profiles during the second switching period ($1 < K_P/K_R < 2$).

P then finds itself in section 4 at the beginning of the third switching period, from where it is collected as product. In order to quantitatively determine the average amount of P entering the reactor we define a dimensionless number α.

$$\alpha = \frac{\text{the amount of P swept out from section 1 during this switching period}}{\text{the amount of P adsorped in section 1 at the beginning of this switching period}} \tag{10}$$

It is apparent that α is the fraction of P recycled during a switching period. If $\alpha = 0$ no product is swept out of section 1 during this switching period, i.e. R and P are completely separated in section 1, which is the case when $K_P/K_R \geq 2$. If $\alpha = 1$ all P adsorbed at the beginning of this switching period is swept out of section 1 and into the reactor with unconverted R during this switching period. This would be true if $K_P/K_R = 1$, and in this case no separation is possible.

In the case $1 < K_P/K_R < 2$, the time when the P concentration front emerges at the outlet of section 1 is

$$t_{bP} = \frac{LA(1-\varepsilon)K_P}{G} \tag{11}$$

i.e. the breakthrough time of P. The rectangular pulse of P in section 1 has moved for 2τ at the end of the second switching period, when the amount of P swept from section 1 is

$$GF_{R0}X(2\tau - t_{bP}) = GF_{R0}X(2t_{bR} - t_{bP}) = F_{R0}XLA(1-\varepsilon)(2K_R - K_P) \tag{12}$$

The total amount of P adsorbed in section 1 at the beginning of the second switching period is

$$GF_{R0}Xt_{bR} = F_{R0}XLA(1-\varepsilon)K_R \tag{13}$$

Substitution of Eqs. (12) and (13) into Eq. (10) gives

$$\alpha = \frac{2K_R - K_P}{K_R}, \quad 1 < K_P/K_R < 2 \tag{14}$$

It is apparent that α, the separative ability of the ideal SCMCR depends only on the adsorption equilibrium constants.

Based on the above analysis, the flow rate of P entering the reactor is $F_{R0}X$, and its duration is $(2t_{bR} - t_{bP})$. The average flow rate of P in the inlet during the entire switching period is

$$\frac{F_{R0}X(2t_{bR} - t_{bP})}{t_{bR}} = \alpha F_{R0}X \tag{15}$$

For convenience, it is assumed that the non-make-up feed flows of R and P during the entire switching period are $F_{R0} = (1 - X)$ and $F_{R0}X\alpha$, respectively. It is easily verified that this assumption has no effect on the average conversion of R in this switching period. Thus, during the second switching period, the flow rates of the feed and the exit streams of the reactor can be obtained. At the end of the second switching period, the rectangular pulses of R and P in section 2 have gas phase flow rates given by $F_{R0}(1 - X)$ and by $F_{R0}X(1 + \alpha)$, respectively, as shown in Fig. 4.

3.1.3. Third switching period

Applying this analysis to the third switching period, the flow rates of R and P at the exit of the reactor during the third switching period are found to be $F_{R0}(1-X)$ and $F_{R0}X(\alpha^2+\alpha+1)$, respectively.

3.1.4. The nth switching period

In the general case, the flow rate of R at the end of the *n*th switching period is

$$F_{Rn} = F_{R0}(1 - X), \quad 0 \leq \alpha < 1 \tag{16}$$

and the flow rate of P is given by

$$F_{Pn} = F_{R0}X\sum \alpha^{(i-1)}, \quad 0 \leq \alpha < 1 \tag{17}$$

Eq. (17) shows how F_{Pn} depends upon the flow rate of R at the reactor inlet, the conversion, X, the number of switching periods and the separation factor. Fig. 5 shows the development of the product concentration normalized by $F_{R0}X$ as a function of switching period, n, for $K_P/K_R = 1.5$ ($\alpha = 0.5$).

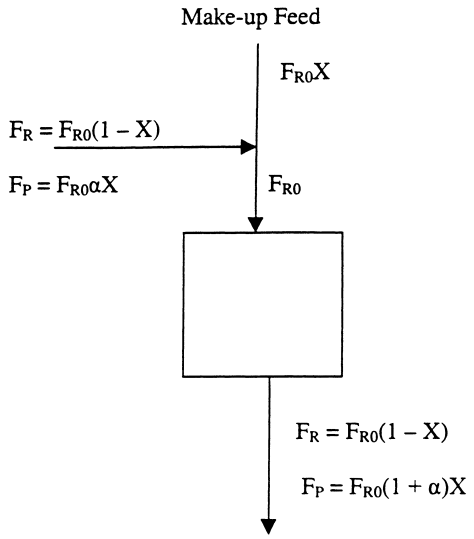

Fig. 4. The reactor feed and exit compositions during the second switching period.

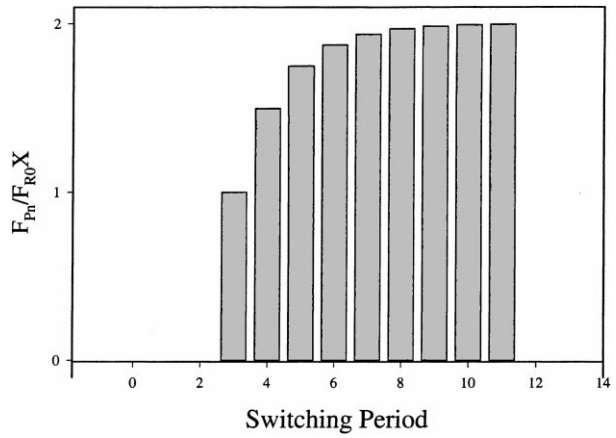

Fig. 5. Development of product profile with increasing switching period for $K_P/K_R = 1.5$ ($\alpha = 0.5$).

The value of $F_{Pn}/F_{R0}X$ increases with increasing n and asymptotically approaches 2.0. It is apparent that the initial transient period is only experimentally distinguishable for at most about 10 switching periods. The asymptote can be calculated from the infinite series given by Eq. (17), since for $-1 < \alpha < +1$ it converges to

$$F_{P\infty} = \frac{F_{R0}}{(1-\alpha)} \tag{19}$$

(Note that $\alpha < 0$ is physically unrealistic here.) The increased concentration of the more strongly adsorbed component which is so apparent in Fig. 5 has been previously reported for a simulated countercurrent moving bed separator [21], and is due to the concentration duty cycle in the product purge column.

Fig. 6 shows the asymptotic value of $F_{Pn}/F_{R0}X$ as a function of a calculated from Eq. (19). The figure reveals that, as separations become more difficult in the sense that K_P/K_R approaches unity, the P in the product take-off will become

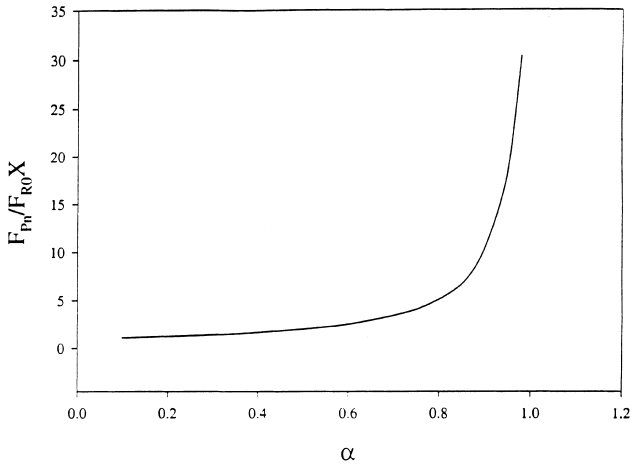

Fig. 6. Dependence of the asymptotic product flow rate, $F_{P,n=\infty}$, relative to make-up feed rate, $F_{R0}X$, on α; $1 < K_P/K_R < 2$.

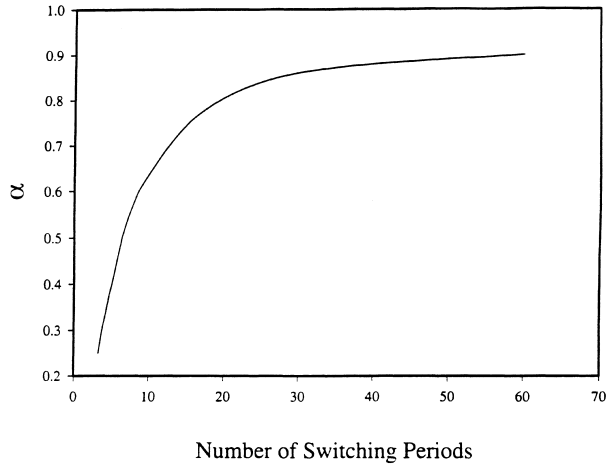

Fig. 7. Number of switching periods for 1% approach to the steady state as a function of α; $1 < K_P/K_R < 2$.

quite large relative to $F_{R0}X$. This occurs because when K_P is not much larger than K_R, the breakthrough times of P and R are not much different, and the time during which P is present in the product stream is only a small fraction of the switching period.

Fig. 7 shows the number of switching periods required for $F_P/F_{R0}X$ to approach to 1% of the asymptote (Eq. (19)) for values of α between 0 and 1. As the separation becomes more difficult n increases, and the function is convex upward, showing that in cases of very difficult separations the transient period may be quite long.

3.2. The reversible reaction

If the reaction of R to form P is now taken to be reversible, R ↔ P, the P that enters the reactor via the internal recycle inhibits the rate of disappearance of R, and the flow rates of R and P emerging from the reactor are different from those for the irreversible reaction. As with the irreversible reaction case above, the makeup feed is adjusted so that the molar flow rate of R entering the reactor (after the mixing point in Fig. 4) is always F_{R0}. Thus, during the first switching period the flow rates of R and P emerging from the reactor are given by $F_R = F_{R0}(1-X)$ and $F_P = F_{R0}X$, as for the irreversible case. It follows that during the second switching period the expressions for F_R and F_P entering the reactor are the same as those shown in Fig. 4. However, here the irreversible and reversible cases diverge due to the inhibiting effect of P on the reaction rate. It can be shown that the reactor effluent concentrations during the second switching period are $F_R = F_{R0}(1-X)(1+\alpha X)$ and $F_P = F_{R0}X(1+\alpha X)$. The former is the flow rate of R entering the reactor during the third switching period, while the flow rate of P entering is given by $F_P = F_{R0}\alpha X(1+\alpha X)$. The exiting flow rates during the third period are $F_R = F_{R0}(1-X)(1+\alpha X+(\alpha X)^2)$ and $F_P = F_{R0}X(1+\alpha X+(\alpha X)^2)$. These expressions can be re-written as $F_R = F_{R0}(1-X)(1-(\alpha X)^3)/(1-\alpha X)$ and

$F_P = F_{R0}X(1-(\alpha X)^3)/(1-\alpha X)$. For the nth switching period these expressions are generalized in Eqs. (20) and (21).

$$F_{Rn} = F_{R0}(1-X)\frac{1-(\alpha X)^n}{1-\alpha X} \tag{20}$$

$$F_{Pn} = F_{R0}X\frac{1-(\alpha X)^n}{1-\alpha X} \tag{21}$$

Since $\alpha X < 1$ for $0 \leq \alpha \leq 1$, Eq. (20) predicts that F_{Rn}/F_{R0} increases from $F_{R1}/F_{R0} = (1-X)$ at $n = 1$ to $F_{R\infty}/F_{R0} = (1-X)/(1-\alpha X)$ at the periodic steady state. To attain the SCMCR performance predicted by the model, it is necessary to provide for adjustment of the make-up feed during the transient period so that $F_{R0}(F_{R0} = F_{Rn} + F_{R\,\text{make-up}})$ remains constant, as required by the model.

Similarly, Eq. (21) predicts that the flow rate of P will increase from $R_{P1} = F_{R0}X$ for $n = 1$, to $F_{P\infty} = F_{R0}X/(1-\alpha)$ at the periodic steady state. As with the irreversible reaction case, the product concentration increases with increasing α, due to the decreasing duty cycle of section 4 as the separation becomes more difficult. There is some advantage to selecting an adsorbent for which the P and R breakthrough times are not too dissimilar, since then the concentration of P is somewhat larger than otherwise, and by collecting product over only the time interval when it is eluting downstream processing can be minimized.

4. Discussion

The flow conditions given by Eqs. (6)–(8), and the switching period of Eq. (9) give optimal performance with respect to reactant conversion and product purity. If they are not adhered to, SCMCR performance suffers. For example, if the switching period is longer than given by Eq. (9), a portion of R breaks through section 2 and enters section 3 in the first switching period. Then at the beginning of the second switching period, this portion of R breaks through the feed section even sooner. For a linear isotherm, the propagation velocity of the front with respect to any concentration of R is constant so at the end of the second switching period this portion of R will be farther from the inlet of section 3. Thus, R "runs ahead of the feed column" and eventually breaks through section 3 where it is removed from the SCMCR. In this scenario, a portion of the R fed in every switching period will be lost in the forthcoming switching periods, and the conversion of R will be less than 100%. If the switching period is shorter than given by Eq. (9), R does not break through column 2 until after the feed point is advanced. The desorption tail will lag behind the feed, eventually reaching section 4 where that portion of R will be swept from the SCMCR. The loss of R causes the conversion to be less than 100%, and also causes the product to be contaminated with R. However, if the optimum flow rates and switching times are employed, R will not be lost from the SCMCR and it can be reacted to extinction.

Reacting R to extinction without losses in the effluent streams implies unit conversion. Furthermore, no reactant loss in the product stream means a high purity product, except for the presence of carrier gas, which must be removed, but which may be a relatively easy separation. These results, which would be expected in a properly designed SCMCR operating according to the ideal model, can only be approached in practice. The effects of axial dispersion and finite mass transfer rates in the adsorbent bed are to broaden the leading and trailing edge of the reactant and product waves, and may lead to some loss of reactant and contamination of product, but the effect is not expected to be large. However, non-linear isotherms can cause significant further deterioration of performance. For example, with a favorable isotherm the concentration front is self-sharpening, which aids performance, but the tail is broadened, which could lead to substantial loss of reactant in a contaminated product stream unless compensated for in SCMCR design. Finally, reactor performance is affected by high energy adsorption sites, which make the purging of section 3 difficult, and may prevent complete removal of product from section 4.

5. Conclusion

Based on the gas–solid flow ratio, optimal operating conditions for a SCMCR capable of high temperature reaction and lower temperature adsorption has been obtained. It has been shown how the optimal flows lead to a SCMCR design in which low conversion per pass reactions, and equilibrium-limited reactions, can be made to proceed to completion. The linear ideal model of chromatography provides analytical solutions for the simulated countercurrent moving bed chromatographic reactor. Explicit algebraic expressions are obtained for the concentration profiles of reactant and product as a function of adsorption equilibrium constants, per pass conversion, switching period and reactant concentration in the internal flows and in the product take-off stream. These analytical expressions provide insight into the fundamentals of SCMCR operation. They are easy to use and provide a useful starting point for further development of reactor design. Knowing the analytical solution for this limiting case provides a useful check on experiments and on numerical solutions of more realistic models. Factors that affect the shape of the moving concentration fronts, such as non-linear adsorption isotherms, finite rates of mass transfer and axial dispersion, will impact SCMCR performance. The ideal model presented here is a convenient and easy benchmark for the effects of these factors on SCMCR performance.

Acknowledgements

This work was supported by a grant from Amoco Chemical Company.

References

[1] A. Ray, A.L. Tonkovich, R. Aris, R.W. Carr, The simulated countercurrent moving bed chromatographic reactor, Chem. Eng. Sci. 45 (1990) 2431.
[2] A. Ray, R.W. Carr, Experimental study of a laboratory scale simulated countercurrent moving bed chromatographic reactor, Chem. Eng. Sci. 50 (1995) 3033.
[3] G.A. Funk, H.W. Dandekar, S.H. Hobbs, US Patent 5,502,248 (1996).
[4] M. Kawase, T.B. Suzuki, K. Inoue, K. Yoshimoto, K. Hashimoto, Increased esterification conversion by application of the simulated moving bed reactor, Chem. Eng. Sci. 51 (1996) 2971.
[5] M. Mazzotti, A. Kruglov, B. Neri, D. Gelosa, M. Morbidelli, A continuous chromatographic reactor: SMBR, Chem. Eng. Sci. 51 (1996) 1827.
[6] A.L. Tonkovich, R.W. Carr, R. Aris, Enhanced C_2 yields from methane oxidative coupling by means of a separative chemical reactor, Science 262 (1993) 221.
[7] A.L. Tonkovich, R.W. Carr, A simulated countercurrent moving bed chromatographic reactor for the oxidative coupling of methane: experimental results, Chem. Eng. Sci. 49 (1994) 4647.
[8] A. Ray, R.W. Carr, R. Aris, The simulated countercurrent moving bed chromatographic reactor: a novel reactor separator, Chem. Eng. Sci. 49 (1994) 469.
[9] A.V. Kruglov, Methanol synthesis in a simulated countercurrent moving bed adsorptive catalytic reactor, Chem. Eng. Sci. 49 (1994) 4699.
[10] A. Ray, R.W. Carr, Numerical simulation of a simulated countercurrent moving bed chromatographic reactor, Chem. Eng. Sci. 50 (1995) 3033.
[11] M. Mazzotti, B. Neri, D. Gelosa, M. Morbidelli, Dynamics of a chromatographic reactor: esterification catalyzed by acidic resins, Ind. Eng. Chem. Res. 36 (1997) 3163.
[12] M. Meurer, U. Altenhöner, J. Strube, H. Schmidt-Traub, J. Chromatogr. A 769 (1997) 71.
[13] C. Migliorini, M. Fillinger, M. Mazzotti, M. Morbidelli, Anal. Simul. Moving Bed Reactors 54 (1999) 2475.
[14] M.C. Bjorklund, R.W. Carr, The simulated countercurrent moving bed chromatographic reactor: a catalytic and separative reactor, Catal. Today 25 (1995) 159.
[15] A.L.Y. Tonkovich, R.W. Carr, Modeling of the simulated countercurrent moving bed chromatographic reactor for the oxidative coupling of methane, Chem. Eng. Sci. 49 (1994) 4657.
[16] A.V. Kruglov, M.C. Bjorklund, R.W. Carr, Optimization of the simulated countercurrent moving bed chromatographic reactor for the oxidative coupling of methane, Chem. Eng. Sci. 51 (1996) 2945.
[17] M.C. Bjorklund, Ph.D. Thesis, University of Minnesota, MN, 1999.
[18] G. Zhong, G. Guiochon, Analytical solution for the linear ideal model of simulated moving bed chromatography, Chem. Eng. Sci. 51 (1996) 4307.
[19] S. Viswanathan, R. Aris, Adv. Chem. Ser. 133 (1974) 191.
[20] D.M. Ruthven, C.B. Ching, Countercurrent and simulated countercurrent adsorption separation processes, Chem. Eng. Sci. 44 (1989) 1011.
[21] B.B. Fish, R.W. Carr, R. Aris, Design and performance of a simulated countercurrent moving bed separator, AIChE J. 39 (1993) 1783.